Atmos. Chem. Phys. Discuss., 13, 19085–19120, 2013
www.atmos-chem-phys-discuss.net/13/19085/2013/
doi:10.5194/acpd-13-19085-2013
© Author(s) 2013. CC Attribution 3.0 License.

Atmospheric Chemistry and Physics Discussions
Open Access

This discussion paper is/has been under review for the journal Atmospheric Chemistry and Physics (ACP). Please refer to the corresponding final paper in ACP if available.

Slower ozone production in Houston, Texas following emission reductions: evidence from Texas Air Quality Studies in 2000 and 2006

W. Zhou[1], D. S. Cohan[1], and B. H. Henderson[2]

[1]Department of Civil and Environmental Engineering, Rice University, Houston, TX 77005, USA
[2]Environmental Engineering Sciences, University of Florida, Gainesville, FL 32611, USA

Received: 13 June 2013 – Accepted: 27 June 2013 – Published: 18 July 2013

Correspondence to: D. S. Cohan (cohan@rice.edu)

Published by Copernicus Publications on behalf of the European Geosciences Union.

Abstract

Airborne measurements from two Texas Air Quality Study (TexAQS) field campaigns have been used to investigate changes of ozone production in Houston, Texas, from 2000 to 2006, a period of major emission reduction measures at petrochemical and other sources. Simultaneous declines in nitrogen oxides ($NO_x = NO + NO_2$) and highly reactive volatile organic compounds (HRVOCs) were observed between the two periods. We simulated HO_x (OH and HO_2) and organic radicals with a box model, the Dynamically Simple Model of Atmospheric Chemical Complexity, constrained by available airborne observations. Parameters such as total radical production, total OH reactivity of VOCs and ozone production rate ($P(O_3)$) are computed to characterize the change of ozone production between 2000 and 2006 in the Houston area. The reduction in HRVOCs led to a decline in total radical production by 20–50 %. Ozone production rates in the Houston area declined by 40–50 % from 2000 to 2006, to which the reduction in NO_x and HRVOCs had large contributions. Despite the significant decline in $P(O_3)$, ozone production efficiency held steady, and VOC-sensitive conditions dominated during times of most rapid ozone formation. Our results highlight the importance of ongoing HRVOC controls to further reduce O_3 levels in the Houston area.

1 Introduction

The Houston metropolitan area has a long history of non-attainment of the US National Ambient Air Quality Standards for ozone (O_3), despite substantial emission reduction efforts since the 1970s (Cowling et al., 2007). Houston ozone events usually occur in spring (April–May) and late summer (August–October) in a bimodal nature. Springtime ozone exceedences tend to occur under post-frontal passage meteorological conditions, while the summertime events often feature continuous high temperature and stagnant meteorology over southeast Texas (Haman et al., 2012; TCEQ, 2007). Favored by these meteorological conditions, large amounts of coemitted NO_x and VOC

ACPD
13, 19085–19120, 2013

from petrochemical facilities in the Houston Ship Channel (HSC) and the nearby urban center lead to high O_3 levels (Fig. 1) (Cowling et al., 2007; Parrish et al., 2009; Ryerson et al., 2003).

Unlike the mobile-dominated hydrocarbon emission compositions in many other metropolitan areas in the US, Houston emissions feature episodic spikes of highly reactive VOCs (HRVOC), such as C_2H_4 and C_3H_6, especially in the HSC region (Kim et al., 2011; Ryerson et al., 2003; Washenfelder et al., 2010). HRVOC emissions result from flaring, fugitive emissions, cooling towers, storage/transport, plastics production, and ethylene and propylene production at petrochemical facilities (Kim et al., 2011). Emission inventories for HRVOC are known to be highly uncertain, due to temporal oscillations in emissions and because emissions from flares and fugitive sources are technically difficult and costly to measure (Kim et al., 2011). Previous studies have concluded that emission inventories in the HSC underestimated HRVOC emissions by at least one order of magnitude (Cowling et al., 2007; Parrish et al., 2009; Ryerson et al., 2003).

The high levels of C_2H_4 and C_3H_6 interacting with NO_x have been shown to foster rapid and efficient O_3 production in Houston (Kleinman et al., 2002a, 2005; Ryerson et al., 2003; Mao et al., 2010). Previous studies have found that $P(O_3)$ in Houston plumes could exceed 100 ppb h^{-1} in contrast to around 20–30 ppb h^{-1} in other metropolitan areas (Kleinman et al., 2002a, 2005).

Despite enormous efforts in curbing HRVOC and NO_x emissions from petrochemical industries and other sources in Houston, peak 8 h O_3 levels have continued to exceed the EPA's 8 h standard (Cowling et al., 2007; Lefer et al., 2010). Meanwhile, up to recently, no study has assessed how the O_3 production and the radical chemistry responded to these emission reductions in the Houston area. Previously, regional transport models were applied to quantify the O_3 trends in the eastern US (Gilliland et al., 2008; Zhou et al., 2013). Using these models to investigate the O_3 trend in Houston area is hindered by the significant underestimation of historical emissions of some HRVOCs from petrochemical industries and the complexity of local meteorology,

ACPD
13, 19085–19120, 2013

such as land-sea breeze and low-level nocturnal jet (Cowling et al., 2007; Parrish et al., 2009).

This study averts the shortcomings of the emissions inventories and meteorological simulations by using observation-based analysis and box modeling to explore trends in O_3 production in the Houston area. Aircraft-based measurements of Houston pollution plumes during Texas Air Quality Studies (TexAQS) in 2000 and 2006 provide a comprehensive data source of air pollutant observations over a time gap of six years, during which major emission controls occurred in Houston (Cowling et al., 2007; Parrish et al., 2009; Ryerson et al., 2003). An observation-constrained box model coupled with a subset of the Master Chemical Mechanism (Jenkin et al., 2003; Saunders et al., 2003) is applied to compute HO_x and RO_x radical concentrations for TexAQS 2000 and 2006.

The second section gives a detailed description of the two TexAQS, the airborne measurement techniques and the metrics of ozone production used in this paper. The third section discusses the changes of measured concentrations, analyzes the changes of the ozone production, and explores the O_3 sensitivity to NO_x and VOC. Finally, we discuss the changes of the ozone production through radical budget analysis, the contributions of NO_x and VOC to ozone production and how the O_3 sensitivity to NO_x and VOC changes due to the emission controls of both species.

2 Methodology

2.1 Texas Air Quality Studies (TexAQS) 2000 and 2006

The Texas Air Quality Studies in 2000 and 2006 were designed to investigate sources and atmospheric processes responsible for the formation and transport of photochemical ozone in eastern Texas and the Houston metropolitan area (Cowling et al., 2007; Parrish et al., 2009). The campaigns were conducted from August to September 2000, and September to October 2006. The rapid O_3 formation and abundant emissions of

ACPD
13, 19085–19120, 2013

HRVOC were identified in the plumes from petrochemical facilities during TexAQS 2000 (Daum et al., 2004; Kleinman et al., 2002a; Ryerson et al., 2003). Both airborne campaigns observed far more HRVOC than would have been expected from the emission inventories, with a smaller gap in 2006 than 2000.

During TexAQS 2000 and 2006, a full spectrum of chemical species were measured by analytical instruments onboard aircraft. During TexAQS 2000, the NCAR aircraft (Electra) performed flights over the Houston area for 10 days (20, 23, 25, 27, 28, 30 August and 1, 6, 7, and 10 September). During TexAQS 2006, the NOAA aircraft (WP-3) performed flights over the Houston area for 11 days (13, 15, 19, 20, 21, 25, 26, and 27 September; 5, 6, and 10 October). The Electra and WP-3 flew at heights of 400–700 m above ground in afternoon hours when sampling pollution plumes, which was well below the typical planetary boundary layer in eastern Texas. A more comprehensive description of the two studies can be found in previous observational studies (Cowling et al., 2007; Parrish et al., 2009; Ryerson et al., 2003).

2.2 Airborne measurement

Various instruments aboard the aircraft measured atmospheric compounds with a range of time resolutions. Inorganic species (O_3, H_2O, NO_x, HNO_3, SO_2, CO, and CO_2), photolysis rates of chemical species, and meteorological parameters were measured at 1 s time resolution. In both years, hydrocarbons (e.g., HRVOC, isoprene) and oxygenated VOCs (e.g., HCHO, peroxyacetyl nitrate (PAN)) were measured with different instruments at different time resolutions. C2–C10 alkanes, C2–C5 alkenes (including C_2H_4 and C_3H_6), ethyne, and C2–C5 aldehydes and ketones were measured via whole air samples (WAS) in canisters. Hydrocarbons in WAS were analyzed in laboratories by gas chromatography mass spectrometry (GCMS) for Non Methane HydroCarbons (NMHC) ($C \geq 3$) and gas chromatography with flame ionization detector (GCFID) for NMHC (C1–C5). There were a total of 726 WAS measurements in 2000 and 814 in 2006.

ACPD
13, 19085–19120, 2013

CC BY

A total of 37 VOC species were measured in 2000 and 2006 (alkene: 12 species; alkane: 12 species; oxygenated species: 13 species). HCHO was measured using tunable diode absorption spectrometry with 1 Hz data. Oxygenated VOCs, such as acetic acid, acetone, acetonitrile, methyl ethyl ketone (MEK), methanol, methyl vinyl ketone (MVK) and methacrolein (MACR) were measured by proton transfer reaction mass spectrometry (PTRMS) every 15 s. PAN was measured by chemical ionization mass spectrometry (CIMS). A full description of all chemical species and the corresponding instruments can be found in Table 1a of Parrish et al. (2009).

Four HRVOC species were identified to be critical in the Houston area due to their high concentration and substantial contribution to the local O_3 formation. They are C_2H_4, C_3H_6, all butene isomers, and 1,3-butadiene. In particular, C_2H_4 and C_3H_6 were the two most important species and were suggested to have the largest impact on ozone production in Houston plumes (Ryerson et al., 2003).

Samples were filtered to remove night-time samples, since O_3 production occurs only during daytime, and samples that lacked valid measurements of key species (NO, NO_2, O_3, and VOCs). After this processing, there were 472 samples in 2000 and 675 samples in 2006.

Because the airborne samples were essentially discrete, cumulative probability distributions are a good option to compare concentrations between 2000 and 2006. The following analysis will frequently discuss the high (top of 10 % samples, e.g., high $P(O_3)$ means the highest 10 % of samples ranked by $P(O_3)$), middle (central 20 %), and low (bottom 10 %) samples. For each subset, the mean value of its samples will be compared between 2000 and 2006.

2.3 Observation-based box model

In TexAQS 2000 and 2006, no valid measurements of HO_x and RO_2 were available for computing the ozone production metrics. A box model, the Dynamically Simple Model of Atmospheric Chemical Complexity (DSMACC) (Emmerson and Evans, 2009) based on the Kinetic Pre-Processor (KPP) (Sandu and Sander, 2006), is applied to compute

ACPD
13, 19085–19120, 2013

the concentrations of HO_x and RO_2. DSMACC has been applied to simulate radicals in other studies (Henderson et al., 2011, 2012; Stone et al., 2010).

The measured photolysis rates of NO_2, O_3 and HCHO are used to constrain photolysis rates in DSMACC. Meteorological inputs include temperature, pressure, and water mixing ratio. The MCM mechanism used in this study is a subset of the comprehensive MCM v3.2 (http://mcm.leeds.ac.uk/MCM/project.htt#New_3.2) and explicitly represents the 37 VOC species measured in TexAQS 2000 and 2006. It contains 3145 chemical reactions, including 3101 organic reactions and 44 inorganic reactions.

The diurnal steady state approach (Olson et al., 2012) is applied to constrain the long-lived species to measurement. Each input point of in-situ data is integrated by the model to find an internally self-consistent diurnal cycle for all computed species to within a given tolerance (< 0.1 %). Predictions are taken from the computed diurnal cycle at the same time of day as the data for direct comparison of radical predictions and measurements.

2.4 Ozone metrics

In evaluating the ozone production, four commonly used ozone metrics are applied in this study. They are total OH reactivity of VOCs (TVOC), ozone production rate ($P(O_3)$), the fraction of radicals removed by reactions with NO_x (L_N/Q), and ozone production efficiency (OPE).

The product of the concentration of a VOC species and its reaction rate with OH, indicates its potential to form first-generation peroxy radicals that facilitate O_3 formation. TVOC is defined in this study as the sum of the OH reactivity of all VOC species and CO (Eq. 1).

$$\mathrm{TVOC} = k_{\mathrm{CO+OH}}[\mathrm{CO}] + \sum_i k_{\mathrm{VOC}_i+\mathrm{OH}}[\mathrm{VOC}_i] \quad (1)$$

Reactions (R) involved in O_3 formation can be grouped into three categories: radical production (Q), chain propagation, and radical termination (L) (Singh, 1995). Radical

ACPD
13, 19085–19120, 2013

production paths generate HO_x and RO_2 radical for chain propagation. The three main radical production reactions are (R1)–(R4) ($Q = 2\times R1 + 2\times R3 + R4$). The radical losses include radical termination by NO_x (R5)–(R8) termed L_N (= R5 + R6 + R7 – R8), and radical-radical combinations to form peroxides (R9)–(R12), termed L_R (= 2 × R9 + 2 × R10 + 2 × R11 + 2 × R12).

Radical production:

$$O_3 + h\nu \rightarrow O(^1D) + O_2 \quad \text{(R1)}$$

$$O(^1D) + H_2O \rightarrow 2OH \quad \text{(R2)}$$

$$HCHO + h\nu \xrightarrow{O_2} 2H_2O + CO \quad \text{(R3)}$$

$$\text{Alkene} + O_3 \rightarrow RO_2 + \cdots \quad \text{(R4)}$$

Radical loss via NO_x reactions:

$$OH + NO_2 \xrightarrow{M} HNO_3 \quad \text{(R5)}$$

$$RO_2 + NO \rightarrow \text{organic nitrate} \quad \text{(R6)}$$

$$RCO_3 + NO_2 \xrightarrow{M} RCO_3NO_2 \quad \text{(R7)}$$

$$RCO_3NO_2 \rightarrow RCO_3 + NO_2 \quad \text{(R8)}$$

Radical loss via radical-radical combination:

$$HO_2 + HO_2 \rightarrow H_2O_2 + O_2 \quad \text{(R9)}$$

$$RO_2 + HO_2 \rightarrow ROOH + O_2 \quad \text{(R10)}$$

$$OH + HO_2 \rightarrow H_2O + O_2 \quad \text{(R11)}$$

$$RO_2 + R'O_2 \rightarrow RO_2R'O_2 \quad \text{(R12)}$$

Since NO_2 photolysis is the dominant reaction known to form O_3 in the troposphere, the ozone production rate is equivalent to the formation rate of NO_2 via two production channels: the reaction of HO_2 with NO and the reactions of organic peroxy radical (RO_2) with NO (Eq. 2). NO_2 is also formed by the reaction of NO with O_3, but this cycling

ACPD
13, 19085–19120, 2013

of NO_x yields no net change in O_3 during daytime. The O_3 loss paths ($L(O_3)$) include O_3 photolysis to generate $O(^1D)$ and subsequent formation of OH radical; the reaction of O_3 with OH and HO_2; and the ozonolysis of VOCs (mainly alkenes). Net_$P(O_3)$ is the difference of $P(O_3)$ and $L(O_3)$ (Eq. 5). FR is the fraction of $O(^1D)$ that generates OH radical rather than returning to ground state odd oxygen.

$$P(O_3) = k_{HO_2+NO}[HO_2][NO] + \sum_i k_{RO_2(i)+NO}[RO_2(i)][NO] \quad (2)$$

$$L(O_3) = \left\{k_{O_3+R}[R] + k_{O_3+HO_2}[HO_2] + k_{O_3+OH}[OH] + FRj(O(^1D))\right\}[O_3] \quad (3)$$

$$FR = \frac{k_{O(^1D)+H_2O}[H_2O]}{k_{O(^1D)+H_2O}[H_2O] + k_{O(^1D)+M}[M]} \quad (4)$$

$$\text{net\_}P(O_3) = P(O_3) - L(O_3) \quad (5)$$

In Eq. (2), k_{HO_2+NO} and $k_{RO_2(i)+NO}$ are the reaction rate coefficients for reactions of HO_2 and RO_2 species with NO. The MCM mechanism in this study has 217 RO_2 species. Since $L(O_3)$ was negligible compared to $P(O_3)$ in polluted daytime samples, we focus our attention on $P(O_3)$ rather than net_$P(O_3)$.

Whether radicals are removed primarily via reactions with NO_x (L_N) or with other radicals (L_R) depends on the relative abundance of NO_x and radicals. L_N/Q is the fraction of radicals removed via the NO_x reactions, assuming that radical production and removal are in balance (Kleinman, 2005). This metric indicates whether the O_3 formation is NO_x- or VOC-sensitive (Kleinman et al., 1997, 2005). When L_N/Q is less than 0.5, it suggests a low NO_x regime and NO_x-sensitive O_3 formation, while larger values of L_N/Q indicate a high NO_x, VOC-sensitive regime.

Ozone production efficiency (OPE) describes the number of molecules of O_3 generated per molecule of NO_x oxidized into reactive nitrogen species (e.g., HNO_3 and organic nitrate) and can be defined in either of two ways. Accumulative OPE compares aggregate O_3 formation and NO_x loss based on the slope of the least-square-fit between O_3 and NO_z ($\equiv NO_y$-NO_x, where NO_y is total reactive nitrogen) observations.

ACPD
13, 19085–19120, 2013

Accumulative OPE gives an upper limit of actual OPE because NO_z loss via deposition is ignored. Instantaneous OPE characterizes current rates of O_3 production per NO_x oxidized based on Eq. (6):

$$\mathrm{OPE} = \mathrm{P(O_3)/L(NO_x)} \tag{6}$$

$$\mathrm{L(NO_x)} = k_{\mathrm{OH+NO_2}}[\mathrm{OH}][\mathrm{NO_2}] + \sum_i k_{\mathrm{NO+RO_2}(i)}[\mathrm{NO}][\mathrm{RO_2}(i)] + \sum_i k_{\mathrm{NO_2+RCO_3}(i)}[\mathrm{NO_2}]\left[\mathrm{RCO_3}(i)\right] - \sum_i k_{\mathrm{RCO_3NO_2}(i)}\left[\mathrm{RCO_3NO_2}(i)\right] \tag{7}$$

3 Results

3.1 Changes of NO_x and HRVOC concentration

In each campaign, the aircraft observed the highest levels of NO_x near the HSC, where many point sources are located, and in the urban center, where densest mobile and area emissions occur (Figs. 1 and 2). The steepest decline in NO_x concentrations was observed at the high end of the distribution (Fig. 3). Meanwhile, the median NO_x concentration declined modestly (17 %), from 2.4 to 2.0 ppb. This is consistent with the sharper emission reductions that are thought to have occurred from point than from area and mobile sources during this period.

Most aircraft observations of high C_2H_4 and C_3H_6 concentrations occurred near the HSC (Fig. 4), indicative of HRVOC emissions from petrochemical plants. It is also clear the hotspots of C_2H_4 and C_3H_6 were less frequent in 2006 than in 2000, suggesting a reduction in HRVOC emissions (Fig. 4). The cumulative distribution functions of both C_2H_4 and C_3H_6 from the HSC (defined here as a rectangular region bordered by 29.5° N/95.6° W and 30.0° N/94.7° W) also show a clear decline of HRVOCs (Fig. 5). The maximal concentrations of C_2H_4 and C_3H_6 were 35 ppb and 89 ppb in 2000, and 18 ppb and 30 ppb in 2006, declines of 48 % and 66 %, respectively. The median con-

ACPD
13, 19085–19120, 2013

centrations of C_2H_4 and C_3H_6 were 2 ppb and 0.5 ppb in 2000, and 1.1 ppb and 0.2 ppb in 2006, declines of 45 % and 51 %, respectively. These results are consistent with the roughly 40 % reductions in HRVOCs reported by previous studies (Cowling et al., 2007; Gilman et al., 2009; Washenfelder et al., 2010).

3.2 Changes of O_3 concentration

Ozone is a secondary pollutant that forms downwind of precursor emission sources, so locations of high ozone vary by day and wind direction (Fig. 6). The maximal aircraft observed O_3 concentrations were 204 ppb in 2000 and 140 ppb in 2006 (Fig. 7). The cumulative distribution of O_3 concentration shows substantial reductions from 2000 to 2006 for high percentile observations, but little change for low percentiles (Fig. 7). This is consistent with Zhou et al. (2013), who found sharper reductions in ozone on peak days than cleaner days in the eastern US.

3.3 Changes of ozone production rate

This section characterizes the decline in ozone production rate ($P(O_3)$) between the two campaigns and the roles of NO_x and VOC emission reductions in these changes. The spatial distribution of $P(O_3)$ in both years indicates the hotspots of $P(O_3)$ primarily occurred in the HSC and the closely surrounding areas, and declined in frequency from 2000 to 2006 (Fig. 6). The maximal $P(O_3)$ declined 68 % from 209 ppb h^{-1} in 2000 to 66 ppb h^{-1} in 2006. The maximal $P(O_3)$ in 2000 occurred in the center of the HSC (NO_x: 29 ppb, TVOC: 67 s^{-1}) while the maximal $P(O_3)$ in 2006 (66 ppb h^{-1}) was observed in the eastern portion of the HSC near Mont Belvieu (NO_x: 8 ppb, TVOC:11 s^{-1}).

More broadly, the average of the highest 10 % of $P(O_3)$ declined 55 % from 59 ppb h^{-1} in 2000 to 26 ppb h^{-1} in 2006 while the average of the middle 20 % $P(O_3)$ of declined 48 % from 12 to 6 ppb h^{-1} (Table 1).The dependence of $P(O_3)$ on NO_x concentration is shown in Fig. 8 for both years. $P(O_3)$ tends to increase with NO_x at low NO_x concentration until a critical point of maximal $P(O_3)$ when NO_x is near 10 ppb. Beyond this point,

ACPD
13, 19085–19120, 2013

CC BY

$P(O_3)$ declines with further increases in NO_x because abundant NO_x rapidly removes OH and peroxy radicals. Even though the measured data in both years cover a wide range of VOC reactivity, generally lower levels of $P(O_3)$ in 2006 for any given level of NO_x reflect the reduction in VOC levels. This is further reflected in $P(O_3)$ peaking at slightly lower levels of NO_x in 2006 (Fig. 8). The downward shift in the data reflects the role of VOC emission reductions, while the leftward shift indicates the impact of NO_x reductions.

The dependence of $P(O_3)$ on TVOC and NO_x concentration in both years is presented in Fig. 9. High levels of NO_x coincide with high levels of TVOC in both years, indicating collocations of NO_x and VOC emission sources. The high $P(O_3)$ had high levels of NO_x and TVOC with the NO_x/TVOC ratio of around 1 : 1 ppb-s for both years (bottom plots of Fig. 9), similar to the results in Lu et al. (2010) and Kleinman et al. (2005). The differences of the $P(O_3)$ between 2000 and 2006 were: (1) more instances of extremely high $P(O_3)$ ($> 70\,\mathrm{ppb\,h^{-1}}$) in 2000, reflecting higher TVOC and NO_x, and (2) for the same levels of NO_x and TVOC ($NO_x < 10$ ppb and TVOC $< 10\,\mathrm{s^{-1}}$), $P(O_3)$ in 2000 tended to be higher than in 2006. For the second difference, one of the reasons is that TVOC does not take account of the fast photolysis of much higher aldehyde and ketone levels in 2000 (e.g., HCHO was 13.9 ppb in 2000 and 7.4 ppb in 2006 for the high $P(O_3)$). Low $P(O_3)$ was associated with the NO_x/TVOC ratio of around 1 : 10. The distribution of measurements from TexAQS 2006 has a long tail of $NO_x < 0.1$ ppb and TVOC $< 1\,\mathrm{s^{-1}}$, which could not be seen in 2000.

3.4 Ozone source and radical budget analysis

Although $P(O_3)$ has been reduced, the relative contribution of VOC sources requires further analysis. This section examines the VOC contributions to $P(O_3)$ by examining radical budget. The contributions of peroxy radicals to $P(O_3)$ at times of rapid O_3 production are summarized in Fig. 10. The HO_2-NO reaction contributed about 60 % of the

ACPD
13, 19085–19120, 2013

CC BY

high $P(O_3)$ in both years, though the rate of this reaction plunged significantly (53 %) from 2000 to 2006.

Among the total 217 RO_2 radicals, 56 species (Table S1 in the Supplement) which contributed more than 95 % of the $P(O_3)$ from the RO_2 and NO reaction are assigned into five groups: $ALKAO_2$, $ALKEO_2$, $CARBO_2$, CH_3O_2, and $ISOPO_2$, approximately reflecting their VOC precursors, i.e., alkanes (C-C), alkenes (C=C), carbonyls, CH_4, and biogenics (Sommarvia et al., 2011). Alkenes correspond to HRVOC while alkanes are mostly anthropogenic saturated hydrocarbons. Carbonyls include a variety of oxygenated VOCs (O-VOCs), such as CH_3CHO, CH_3COCH_3, MEK, and MVK, which may be formed from the OH-oxidation of HRVOCs, isoprene and other long-chain hydrocarbons.

Among the NO and RO_2 reactions, the two largest components were $ALKEO_2$ and $CARBO_2$, the combination of which contributed roughly 25 % of the high $P(O_3)$ in both years. CH_3O_2 contributed only a small amount (8.1 % (2000) and 11.3 % (2006)) to $P(O_3)$ in this study domain in contrast to the rural atmosphere where CH_3O_2 usually contributes about 30 % of $P(O_3)$ (Sommariva et al., 2011). Alkanes and biogenic VOCs had very small contributions to $P(O_3)$ in the two years.

$P(O_3)$ from RO_2 radicals of alkanes, carbonyls, and HRVOCs declined dramatically from 2000 to 2006: 53 % for $ALKO_2$, 39 % for $CARBO_2$, and 71 % for $ALKEO_2$. Meanwhile, little change was observed from $ISOPO_2$ originating from largely biogenic isoprene, and CH_3O_2 originating from long-lived methane which has numerous biogenic and anthropogenic sources globally. This is consistent with the decline in anthropogenic VOCs and HRVOC between these periods.

From the $P(O_3)$ source analysis, we have seen that the HO_2 term was the dominant contributor to the high $P(O_3)$, and its reduction led to the decline of $P(O_3)$ from 2000 to 2006. The HO_2 radical budget for the high $P(O_3)$ samples is examined to investigate sources of HO_2 and how they changed over this period. Total HO_2 production rate declined by 53 % from $3.77 \times 10^8\,cm^{-3}\,s^{-1}$ in 2000 to $1.75 \times 10^8\,cm^{-3}\,s^{-1}$ in 2006. Even though HO_2NO_2 formation and decomposition has large weights compared to

ACPD
13, 19085–19120, 2013

other HO_2 loss and production processes (Fig. 11), the net of HO_2NO_2 formation and decomposition was only a minor component (3.4–4.5 %) of the HO_2 budget in both years.

Excluding the HO_2NO_2 formation and decomposition, HCHO+OH (18 %), HYPROPO ($OHCH_2C(O\bullet)CH_3$) photolysis (14 %), and HCHO photolysis (13 %) contributed about half of the HO_2 production rate in 2000. In 2006, HCHO+OH (19.1 %), and HCHO photolysis (14.0 %) had similar contributions to the HO_2 production rate while the contribution of HYPROPO to the HO_2 production rate declined significantly to 8 %.

HYPROPO is predominantly produced from the reaction of C_3H_6 with OH in the MCM. The sources of HCHO in the Houston area have been substantially debated. A few studies using regression analysis of HCHO with primary and secondary pollutants have argued that the primary emission has a larger contribution to ground-level HCHO concentrations than secondary formation (Buzcu Guven and Olaguer, 2011; Olaguer et al., 2009; Rappenglück et al., 2010). However, a comprehensive chemical analysis of airborne HCHO coupled with ground HCHO measurements and emissions data concluded that HCHO in HGB was predominantly formed from VOC oxidation (Parrish et al., 2012). We used the same airborne data as Parrish et al. (2009). A careful examination of all airborne data in this study did not find HCHO-only spikes but observed that the enhancements of HCHO were strongly associated with those of O_3. These two facts are consistent with the claim of Parrish et al. (2012) that HCHO primarily (92 %) resulted from HRVOC oxidation. Following this assumption, 40 % of HO_2 production can be attributed to HRVOC as a conservative estimate in both years.

Other minor contributing reactions include the oxidation of $HOCH_2CH_2O$, C_2H_5O, $HOCH_2CO_3$, and IPROPOLO ($OHCH(CH_3)CH_2(O\bullet)$) reactions, contributing a total 15 % of HO_2 production rate. These oxygenated intermediate species and radicals could partially be HRVOC oxidation products. Thus, we conclude that HRVOC played a major role in HO_2 production in both years, and its emission reduction was key to the decline of HO_2 radical and $P(O_3)$ between the two campaigns.

ACPD
13, 19085–19120, 2013

3.5 O_3 sensitivity to NO_x and TVOC

L_N/Q is indicative of whether O_3 formed in a NO_x- or VOC-sensitive regime. In both years, the value of L_N/Q spanned a wide range (0–1), suggesting the airborne data represented a wide variety of O_3 formation chemistry from places in the immediate vicinity of emission sources in HSC to the background atmosphere (Fig. 12). At low NO_x levels (≤ 1 ppb) in both years, low L_N/Q (0–0.5) suggested a NO_x-sensitive O_3 formation. Higher L_N/Q (≥ 0.5) indicated a VOC-sensitive O_3 formation under higher NO_x levels. The L_N/Q distribution over the NO_x-TVOC space presented in this study is similar to the distribution from the G-1 airborne data during TexAQS 2000 (Kleinman et al., 2005). L_N/Q for the high $P(O_3)$ samples (bottom plots of Fig. 12) indicate a strongly VOC-sensitive O_3 formation regime while no significant changes existed between 2000 and 2006, reflecting the simultaneous declines in NO_x and VOCs.

3.6 Ozone production efficiency

The instantaneous OPE computed from the DSMACC box model considers only the chemical processes and not physical ones such as deposition. As indicated in Eq. (6), instantaneous OPE is $P(O_3)$ divided by $L(NO_x)$. NO_x loss ($L(NO_x)$) is mainly from the reaction of NO_2 with OH (R4) and RCO_3 (R6)–(R7), and the reaction of NO with RO_2 (R5). The average and maximal instantaneous OPEs were consistent with those in other regions (Griffin et al., 2004; Kleinman et al., 2002b).

While cloud processing could bias OPE high by rapidly removing NO_y (Zhou et al., 2012), MODIS satellite images indicate mostly cloud-free conditions in the immediate vicinity of the transects. High OPEs (8–15) were always observed in the diluted industrial plume transects over the isoprene-rich northern rural area while OPEs in urban and industrial plumes transported southerly tended to be lower (5–7). When both NO_x and VOCs declined significantly by roughly 30–40 %, the accumulative OPEs did not show clear differences between 2000 and 2006. An example was the closely matched OPEs with the highest O_3 between 2000 and 2006 even though both O_3 and NO_z came

ACPD
13, 19085–19120, 2013

down substantially (Fig. 13). The instantaneous OPE is not directly comparable to the accumulative OPE because the instantaneous OPE involves only chemical reactions and covers a small temporal and spatial subset of data (Griffin et al., 2004).

4 Discussion and conclusion

Airborne measurements from TexAQS 2000 and 2006 have been used to investigate the change of ozone production in Houston. A box model, DSMACC, has been applied to simulate HO_x and RO_2 radicals with the airborne data. Total radical concentration, $P(O_3)$, L_N/Q and OPE are compared between 2000 and 2006 at all levels. A comprehensive summary of the comparison of these parameters is presented in Table 1. The parameters shown in Table 1 for 2000 are consistent with the results from the other airborne measurement (118 samples) by the G-1 aircraft during TexAQS 2000 (Kleinman et al., 2005).

Decreased HRVOC emissions are the main cause of reduced radical production (Q in Table 1). Total radicals declined about 51 % and 21 % for the high and middle $P(O_3)$, reflecting the deeper reductions in the most polluted plumes. HO_2 and RO_2 radicals had similar extents of declines. RO_2 sources were dominated by alkenes (HRVOCs) (30–50 %) and carbonyls (30–40 %). HO_2 radicals were mainly formed from the HCHO reactions and the HRVOC oxidation products. Our analysis linked the radical decline to the decline in HRVOC emissions. More than 40 % of HO_2 production for the high $P(O_3)$ samples could be attributed to HRVOC in both years, and the decline in HRVOCs was critical to the overall decline in radical levels. The simultaneous declines in NO_x and radicals led to a 40–50 % decline in ozone production rate in the Houston area at times of high and middle $P(O_3)$ (Table 1). $P(O_3)$ declined at all levels of NO_x, reflecting the reduction in VOC levels.

The periods of most rapid ozone production, were characterized by VOC-sensitive conditions, as indicated by high levels of L_N/Q in samples with high $P(O_3)$ in both years. Meanwhile, the O_3 sensitivity for the middle $P(O_3)$ shifted from the transition regime

ACPD
13, 19085–19120, 2013

(L_N/Q = 0.5) to the VOC-sensitive regime (L_N/Q = 0.7). OPE remained at similar high levels (5–15) in both years, due to the similar rates of declines in NO_x and TVOC.

The results from this study have relevance to policy. Times of most rapid ozone production in the Houston area were found to be VOC-sensitive, and HRVOCs were dominant precursors of peroxy radicals. This suggests the importance of ongoing reductions in HRVOC emissions to achieve further reductions in O_3. Nevertheless, NO_x-sensitive conditions continued to be observed at some times and locations and OPE remained high, indicating a need for a balanced approach to emission reductions for a region characterized by transitional and nonlinear ozone formation conditions (Xiao et al., 2010).

Supplementary material related to this article is available online at: http://www.atmos-chem-phys-discuss.net/13/19085/2013/acpd-13-19085-2013-supplement.pdf.

Acknowledgements. The work of Wei Zhou and Daniel Cohan was funded by National Science Foundation CAREER Award Grant 087386. We thank Mat Evans of York University in UK for providing DSMACC box model and ropa.pro, a radical budget analysis tool. We thank the NOAA ESRL for providing the TexAQS 2000 and 2006 airborne measurement data.

References

Buzcu Guven, B. and Olaguer, E. P.: Ambient formaldehyde source attribution in Houston during TexAQS II and TRAMP, Atmos. Environ., 45, 4272–4280, 2011.

Cowling, E. B., Furiness, C., Dimitriades, B., Parrish, D., and Estes, M.: Final Rapid Science Synthesis Report: Findings from the Second Texas Air Quality Study Southern Oxidants Study Office of the Director at North Carolina State University Location: Raleigh, NC, USA, 2007.

ACPD
13, 19085–19120, 2013

Daum, P. H., Kleinman, L. I., Springston, S. R., Nunnermacker, L. J., Lee, Y. N., Weinstein-Lloyd, J., Zheng, J., and Berkowitz, C. M.: Origin and properties of plumes of high ozone observed during the Texas 2000 Air Quality Study (TexAQS 2000), J. Geophys. Res.-Atmos., 109, D17306, doi:10.1029/2003jd004311, 2004.

Emmerson, K. M. and Evans, M. J.: Comparison of tropospheric gas-phase chemistry schemes for use within global models, Atmos. Chem. Phys., 9, 1831–1845, doi:10.5194/acp-9-1831-2009, 2009.

Gilliland, A. B., Hogrefe, C., Pinder, R. W., Godowitch, J. M., Foley, K. L., and Rao, S. T.: Dynamic evaluation of regional air quality models: assessing changes in O_3 stemming from changes in emissions and meteorology, Atmos. Environ., 42, 5110–5123, 2008.

Gilman, J. B., Kuster, W. C., Goldan, P. D., Herndon, S. C., Zahniser, M. S., Tucker, S. C., Brewer, W. A., Lerner, B. M., Williams, E. J., Harley, R. A., Fehsenfeld, F. C., Warneke, C., and de Gouw, J. A.: Measurements of volatile organic compounds during the 2006 TexAQS/GoMACCS campaign: Industrial influences, regional characteristics, and diurnal dependencies of the OH reactivity, J. Geophys. Res.-Atmos., 114, D00F06, doi:10.1029/2008jd011525, 2009.

Griffin, R. J., Johnson, C. A., Talbot, R. W., Mao, H., Russo, R. S., Zhou, Y., and Sive, B. C.: Quantification of ozone formation metrics at Thompson Farm during the New England Air Quality Study (NEAQS) 2002, J. Geophys. Res.-Atmos., 109, D24302, doi:10.1029/2004jd005344, 2004.

Haman, C. L., Lefer, B., and Morris, G. A.: Seasonal variability in the diurnal evolution of the boundary layer in a near-coastal urban environment, J. Atmos. Ocean. Tech., 29, 697–710, doi:10.1175/jtech-d-11-00114.1, 2012.

Henderson, B. H., Pinder, R. W., Crooks, J., Cohen, R. C., Hutzell, W. T., Sarwar, G., Goliff, W. S., Stockwell, W. R., Fahr, A., Mathur, R., Carlton, A. G., and Vizuete, W.: Evaluation of simulated photochemical partitioning of oxidized nitrogen in the upper troposphere, Atmos. Chem. Phys., 11, 275–291, doi:10.5194/acp-11-275-2011, 2011.

Henderson, B. H., Pinder, R. W., Crooks, J., Cohen, R. C., Carlton, A. G., Pye, H. O. T., and Vizuete, W.: Combining Bayesian methods and aircraft observations to constrain the HO + NO_2 reaction rate, Atmos. Chem. Phys., 12, 653–667, doi:10.5194/acp-12-653-2012, 2012.

Jenkin, M. E., Saunders, S. M., Wagner, V., and Pilling, M. J.: Protocol for the development of the Master Chemical Mechanism, MCM v3 (Part B): tropospheric degradation of aromatic

volatile organic compounds, Atmos. Chem. Phys., 3, 181–193, doi:10.5194/acp-3-181-2003, 2003.

Kim, S.-W., McKeen, S. A., Frost, G. J., Lee, S.-H., Trainer, M., Richter, A., Angevine, W. M., Atlas, E., Bianco, L., Boersma, K. F., Brioude, J., Burrows, J. P., de Gouw, J., Fried, A., Gleason, J., Hilboll, A., Mellqvist, J., Peischl, J., Richter, D., Rivera, C., Ryerson, T., te Lintel Hekkert, S., Walega, J., Warneke, C., Weibring, P., and Williams, E.: Evaluations of NO_x and highly reactive VOC emission inventories in Texas and their implications for ozone plume simulations during the Texas Air Quality Study 2006, Atmos. Chem. Phys., 11, 11361–11386, doi:10.5194/acp-11-11361-2011, 2011.

Kleinman, L. I.: The dependence of tropospheric ozone production rate on ozone precursors, Atmos. Environ., 39, 575–586, 2005.

Kleinman, L. I., Daum, P. H., Lee, J. H., Lee, Y.-N., Nunnermacker, L. J., Springston, S. R., Newman, L., Weinstein-Lloyd, J., and Sillman, S.: Dependence of ozone production on NO and hydrocarbons in the troposphere, Geophys. Res. Lett., 24, 2299–2302, doi:10.1029/97gl02279, 1997.

Kleinman, L. I., Daum, P. H., Imre, D., Lee, Y. N., Nunnermacker, L. J., Springston, S. R., Weinstein-Lloyd, J., and Rudolph, J.: Ozone production rate and hydrocarbon reactivity in 5 urban areas: a cause of high ozone concentration in Houston, Geophys. Res. Lett., 29, 1467, doi:10.1029/2001gl014569, 2002a.

Kleinman, L. I., Daum, P. H., Lee, Y.-N., Nunnermacker, L. J., Springston, S. R., Weinstein-Lloyd, J., and Rudolph, J.: Ozone production efficiency in an urban area, J. Geophys. Res.-Atmos., 107, 4733, doi:10.1029/2002jd002529, 2002b.

Kleinman, L. I., Daum, P. H., Lee, Y. N., Nunnermacker, L. J., Springston, S. R., Weinstein-Lloyd, J., and Rudolph, J.: A comparative study of ozone production in five US metropolitan areas, J. Geophys. Res.-Atmos., 110, D02301, doi:10.1029/2004jd005096, 2005.

Lefer, B., Rappenglück, B., Flynn, J., and Haman, C.: Photochemical and meteorological relationships during the Texas-II Radical and Aerosol Measurement Project (TRAMP), Atmos. Environ., 44, 4005–4013, 2010.

Lu, K., Zhang, Y., Su, H., Brauers, T., Chou, C. C., Hofzumahaus, A., Liu, S. C., Kita, K., Kondo, Y., Shao, M., Wahner, A., Wang, J., Wang, X., and Zhu, T.: Oxidant ($O_3 + NO_2$) production processes and formation regimes in Beijing, J. Geophys. Res.-Atmos., 115, D07303, doi:10.1029/2009jd012714, 2010.

ACPD
13, 19085–19120, 2013

Mao, J., Ren, X., Chen, S., Brune, W. H., Chen, Z., Martinez, M., Harder, H., Lefer, B., Rappenglück, B., Flynn, J., and Leuchner, M.: Atmospheric oxidation capacity in the summer of Houston 2006: comparison with summer measurements in other metropolitan studies, Atmos. Environ., 44, 4107–4115, 2010.

Olaguer, E. P., Rappenglück, B., Lefer, B., Stutz, J., Dibb, J., Griffin, R., Brune, W. H., Shauck, M., Buhr, M., Jeffries, H., Wiuete, W., and Pinto, J. P.: Deciphering the role of radical precursors during the Second Texas Air Quality Study, J. Air. Waste Mange Assoc., 59, 1258–1277, doi:10.3155/1047-3289.59.11.1258, 2009.

Olson, J. R., Crawford, J. H., Brune, W., Mao, J., Ren, X., Fried, A., Anderson, B., Apel, E., Beaver, M., Blake, D., Chen, G., Crounse, J., Dibb, J., Diskin, G., Hall, S. R., Huey, L. G., Knapp, D., Richter, D., Riemer, D., Clair, J. St., Ullmann, K., Walega, J., Weibring, P., Weinheimer, A., Wennberg, P., and Wisthaler, A.: An analysis of fast photochemistry over high northern latitudes during spring and summer using in-situ observations from ARCTAS and TOPSE, Atmos. Chem. Phys., 12, 6799–6825, doi:10.5194/acp-12-6799-2012, 2012.

Parrish, D. D., Allen, D. T., Bates, T. S., Estes, M., Fehsenfeld, F. C., Feingold, G., Ferrare, R., Hardesty, R. M., Meagher, J. F., Nielsen-Gammon, J. W., Pierce, R. B., Ryerson, T. B., Seinfeld, J. H., and Williams, E. J.: Overview of the Second Texas Air Quality Study (TexAQS II) and the Gulf of Mexico Atmospheric Composition and Climate Study (GoMACCS), J. Geophys. Res.-Atmos., 114, D00F13, doi:10.1029/2009jd011842, 2009.

Parrish, D. D., Ryerson, T. B., Mellqvist, J., Johansson, J., Fried, A., Richter, D., Walega, J. G., Washenfelder, R. A., de Gouw, J. A., Peischl, J., Aikin, K. C., McKeen, S. A., Frost, G. J., Fehsenfeld, F. C., and Herndon, S. C.: Primary and secondary sources of formaldehyde in urban atmospheres: Houston Texas region, Atmos. Chem. Phys., 12, 3273–3288, doi:10.5194/acp-12-3273-2012, 2012.

Rappenglück, B., Dasgupta, P. K., Leuchner, M., Li, Q., and Luke, W.: Formaldehyde and its relation to CO, PAN, and SO_2 in the Houston-Galveston airshed, Atmos. Chem. Phys., 10, 2413–2424, doi:10.5194/acp-10-2413-2010, 2010.

Ryerson, T. B., Trainer, M., Angevine, W. M., Brock, C. A., Dissly, R. W., Fehsenfeld, F. C., Frost, G. J., Goldan, P. D., Holloway, J. S., Hübler, G., Jakoubek, R. O., Kuster, W. C., Neuman, J. A., Nicks Jr., D. K., Parrish, D. D., Roberts, J. M., Sueper, D. T., Atlas, E. L., Donnelly, S. G., Flocke, F., Fried, A., Potter, W. T., Schauffler, S., Stroud, V., Weinheimer, A. J., Wert, B. P., Wiedinmyer, C., Alvarez, R. J., Banta, R. M., Darby, L. S., and Senff, C. J.: Effect of petrochemical industrial emissions of reactive alkenes and NO_x on tropospheric ozone for-

ACPD
13, 19085–19120, 2013

mation in Houston, Texas, J. Geophys. Res.-Atmos., 108, 4249, doi:10.1029/2002jd003070, 2003.

Sandu, A. and Sander, R.: Technical note: Simulating chemical systems in Fortran90 and Matlab with the Kinetic PreProcessor KPP-2.1, Atmos. Chem. Phys., 6, 187–195, doi:10.5194/acp-6-187-2006, 2006.

Saunders, S. M., Jenkin, M. E., Derwent, R. G., and Pilling, M. J.: Protocol for the development of the Master Chemical Mechanism, MCM v3 (Part A): tropospheric degradation of non-aromatic volatile organic compounds, Atmos. Chem. Phys., 3, 161–180, doi:10.5194/acp-3-161-2003, 2003.

Sommariva, R., Bates, T., Bon, D., Brookes, D., Gouw, J., Gilman, J., Herndon, S., Kuster, W., Lerner, B., Monks, P., Osthoff, H., Parker, A., Roberts, J., Tucker, S., Warneke, C., Williams, E., Zahniser, M., and Brown, S.: Modelled and measured concentrations of peroxy radicals and nitrate radical in the US Gulf Coast region during TexAQS 2006, J. Atmos. Chem., 68, 331–362, doi:10.1007/s10874-012-9224-7, 2011.

Singh, H. B.: Composition, Chemistry, and Climate of the Atmosphere, 1st edn., Wiley, New York, 1995

Stone, D., Evans, M. J., Commane, R., Ingham, T., Floquet, C. F. A., McQuaid, J. B., Brookes, D. M., Monks, P. S., Purvis, R., Hamilton, J. F., Hopkins, J., Lee, J., Lewis, A. C., Stewart, D., Murphy, J. G., Mills, G., Oram, D., Reeves, C. E., and Heard, D. E.: HO_x observations over West Africa during AMMA: impact of isoprene and NO_x, Atmos. Chem. Phys., 10, 9415–9429, doi:10.5194/acp-10-9415-2010, 2010.

TCEQ: 2006 TEXAQS/GoMACCS Comprehensive Meteorological Analysis of TexAQS II data, Austin, Texas, USA Issuing organization: Texas Commission on Environmental Quality, 2007.

Washenfelder, R. A., Trainer, M., Frost, G. J., Ryerson, T. B., Atlas, E. L., de Gouw, J. A., Flocke, F. M., Fried, A., Holloway, J. S., Parrish, D. D., Peischl, J., Richter, D., Schauffler, S. M., Walega, J. G., Warneke, C., Weibring, P., and Zheng, W.: Characterization of NO_x, SO_2, ethene, and propene from industrial emission sources in Houston, Texas, J. Geophys. Res.-Atmos., 115, D16311, doi:10.1029/2009jd013645, 2010.

Xiao, X., Cohan, D. S., Byun, D. W., and Ngan, F.: Highly nonlinear ozone formation in the Houston region and implications for emission controls, J. Geophys. Res.-Atmos., 115, D23309, doi:10.1029/2010jd014435, 2010.

ACPD
13, 19085–19120, 2013

Zhou, W., Cohan, D. S., Pinder, R. W., Neuman, J. A., Holloway, J. S., Peischl, J., Ryerson, T. B., Nowak, J. B., Flocke, F., and Zheng, W. G.: Observation and modeling of the evolution of Texas power plant plumes, Atmos. Chem. Phys., 12, 455–468, doi:10.5194/acp-12-455-2012, 2012.

Zhou, W., Cohan, D. S., and Napelenok, S. L.: Reconciling NO_x emissions reductions and ozone trends in the US, 2002–2006, Atmos. Environ., 70, 236–244, 2013.

ACPD
13, 19085–19120, 2013

Table 1. Parameters of O_3 production for the high, middle and low $P(O_3)$ samples for 2000 and 2006*.

Parameters	High $P(O_3)$		Middle $P(O_3)$		Low $P(O_3)$	
	2000	2006	2000	2006	2000	2006
$P(O_3)$ (ppb h^{-1})	58.9	26.4	12.4	6.4	0.8	0.3
O_3 (ppb)	123	75	80	61	66	57
Q (ppb h^{-1})	12.5	6.1	2.8	2.2	1.1	0.4
NO_x (ppb)	14.1	7.2	4.6	3.2	0.3	1.0
TVOC (s^{-1})	12.0	6.7	4.2	2.8	1.9	1.7
L_N/Q	0.8	0.9	0.5	0.7	0.2	0.2

* All values of parameters are the mean for the subset. The parameters chosen here follow Table 4 of Kleinman et al. (2005). High $P(O_3)$ refers to the top 10 % samples ranked by $P(O_3)$; middle $P(O_3)$ is the central 20 % samples; and low $P(O_3)$ refers to the bottom 10 % samples.

ACPD
13, 19085–19120, 2013

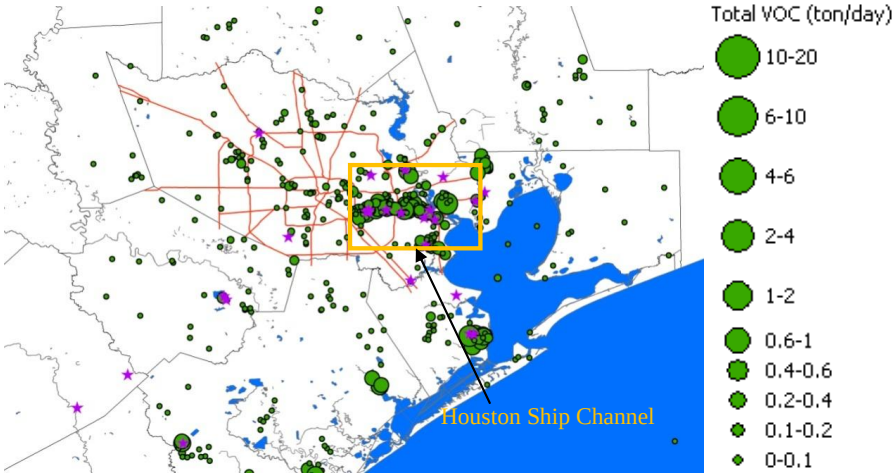

Fig. 1. Map centered on the Houston metropolitan area, showing highways (red lines) and NO_x and VOC point sources. NO_x point sources from Continuous Emission Monitoring System (CEMS) are shown by purple stars. Green circles indicate total VOC emissions rate (tons/day) from point sources during TexAQS 2006 (data source: Texas Commission on Environmental Quality). The Houston Ship Channel is identified by a yellow frame.

ACPD
13, 19085–19120, 2013

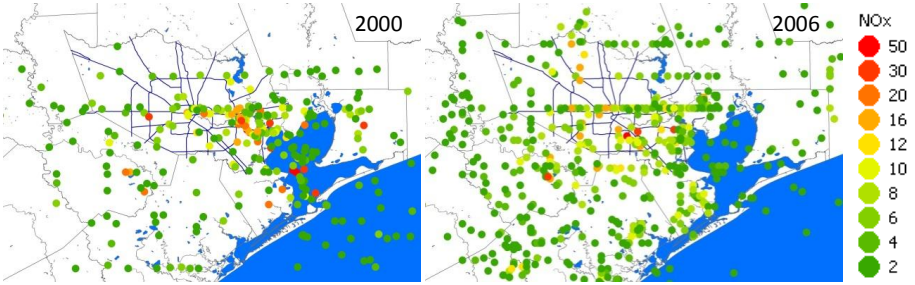

Fig. 2. The spatial distribution of NO_x concentrations observed by aircraft during TexAQS 2000 and 2006.

ACPD
13, 19085–19120, 2013

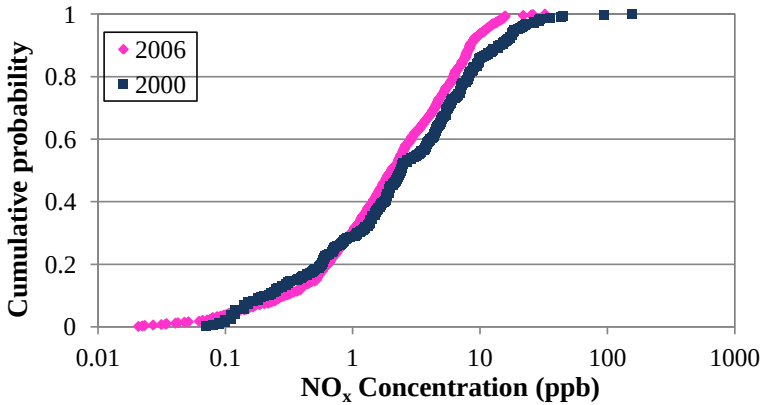

Fig. 3. The cumulative probability distribution of NO_x concentrations in 2000 and 2006.

ACPD
13, 19085–19120, 2013

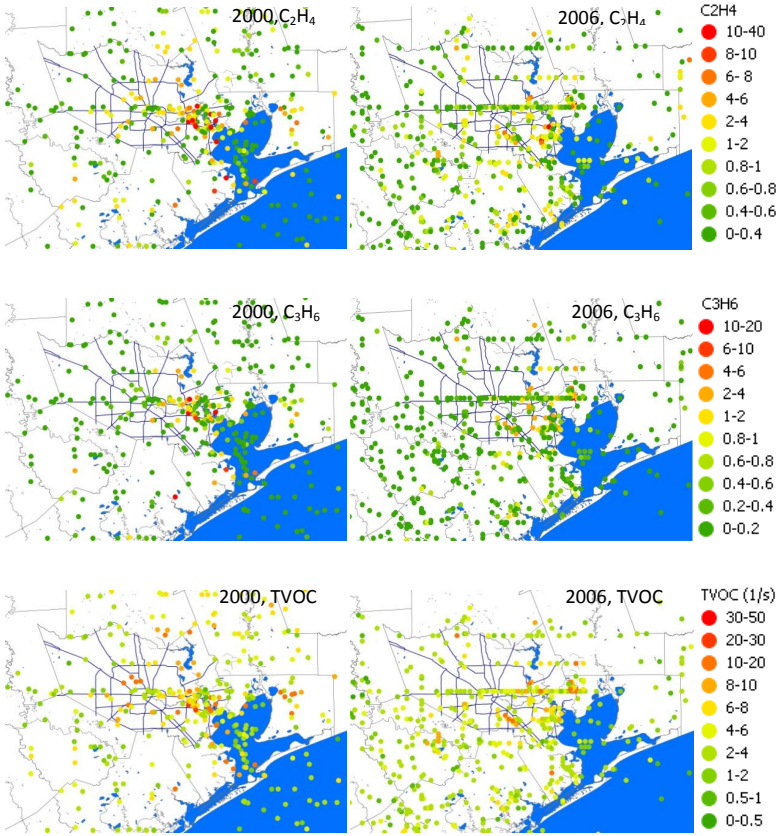

Fig. 4. Spatial distribution of C_2H_4 (top), C_3H_6 (middle), and total VOC reactivity (TVOC) (bottom) in 2000 and 2006.

ACPD
13, 19085–19120, 2013

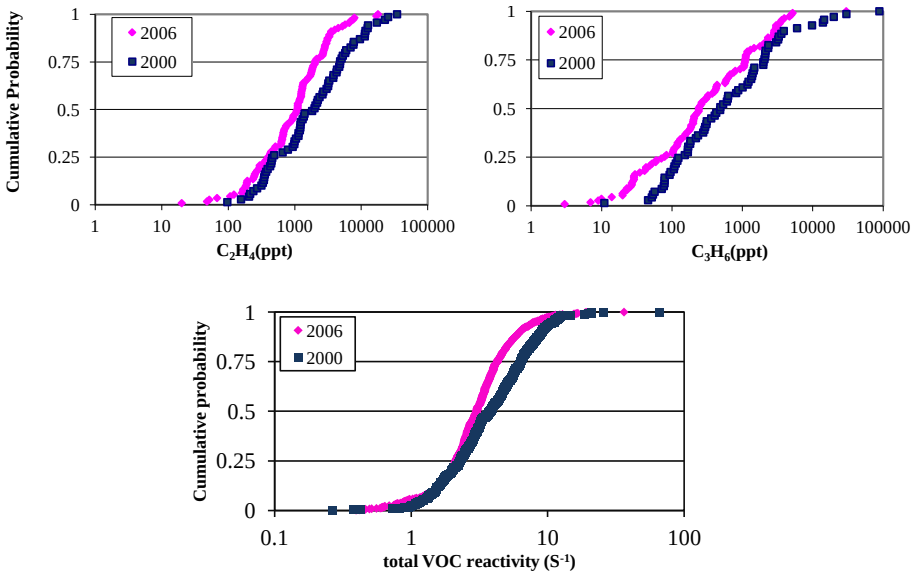

Fig. 5. The cumulative probability distribution of C_2H_4 (top left), C_3H_6 (top right), and total VOC reactivity (bottom) in 2000 and 2006.

ACPD
13, 19085–19120, 2013

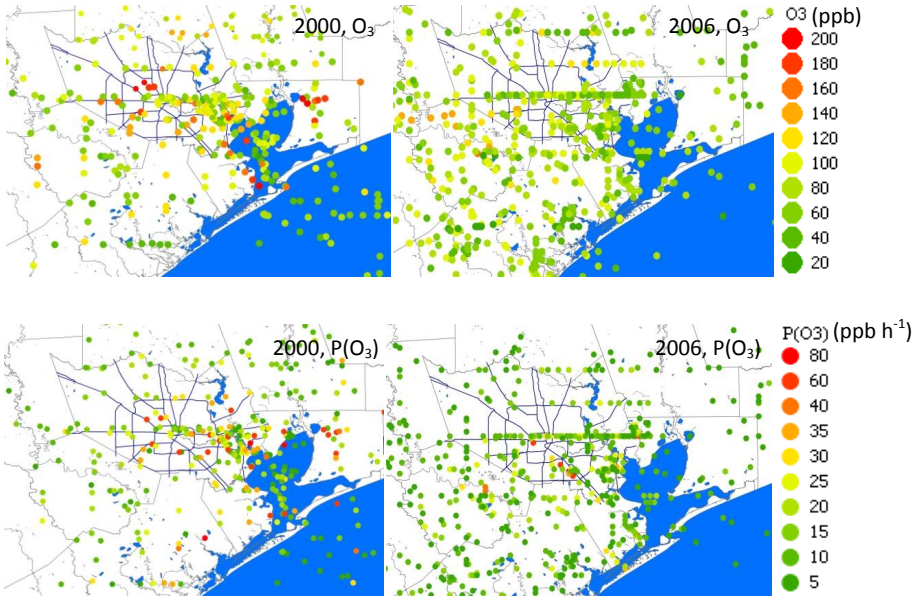

Fig. 6. Spatial distribution of O_3 (top) and $P(O_3)$ (bottom) during TexAQS 2000 and 2006.

ACPD
13, 19085–19120, 2013

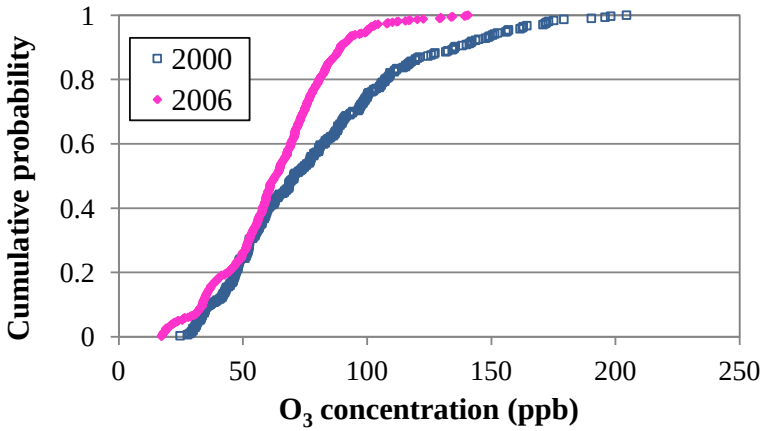

Fig. 7. The cumulative probability distribution of O_3 in 2000 and 2006.

ACPD
13, 19085–19120, 2013

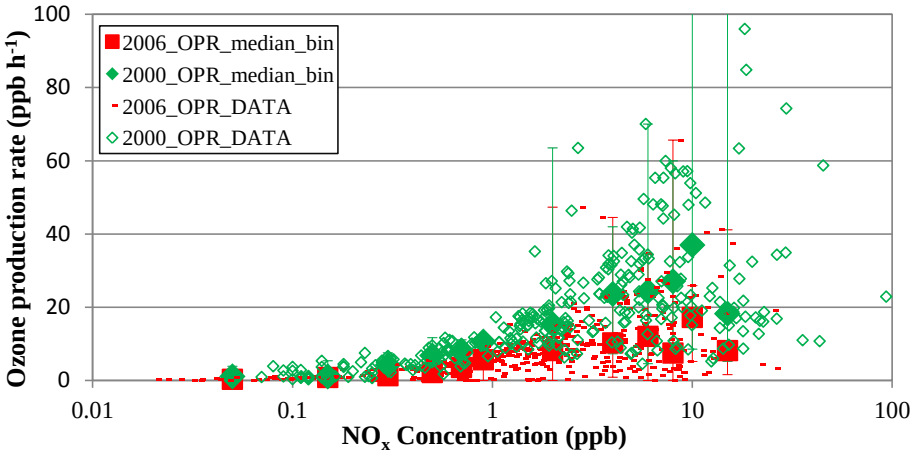

Fig. 8. $P(O_3)$ as a function of NO_x concentration for 2000 and 2006. The filled green diamonds and red squares are the median values of each bin segment. NO_x concentration from 0.01 to 0.1 ppb has one bin, 0.1–1.0 ppb has 5 bins, 1–10 ppb has 5 bins, > 10 ppb has one bin.

ACPD
13, 19085–19120, 2013

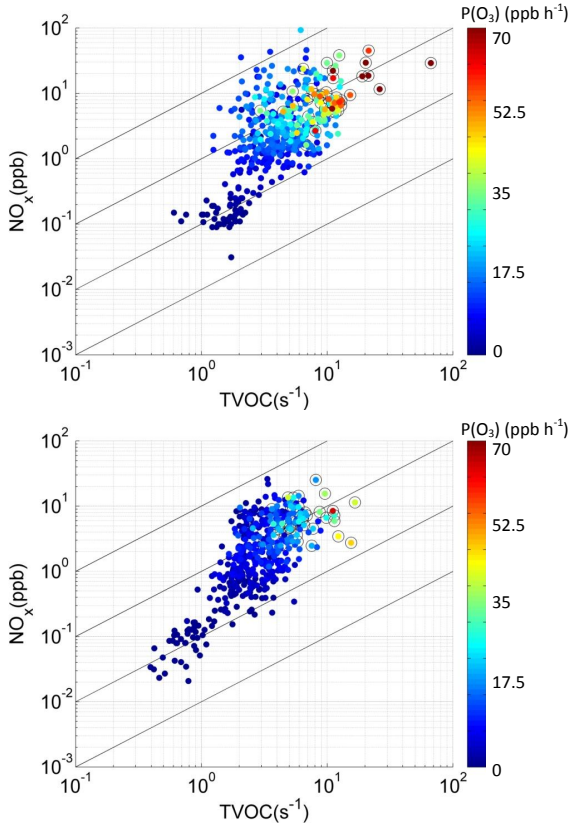

Fig. 9. The dependence of $P(O_3)$ shown in color scale on total VOC reactivity (TVOC) and NO_x concentration for both 2000 and 2006. In the top plots, samples of high $P(O_3)$ are marked by empty circles. Each diagonal line is associated with a constant TVOC to NO_x ratio (from top to bottom, TVOC/NO_x = 10 : 1, 1 : 1, 1 : 10, 1 : 100).

ACPD
13, 19085–19120, 2013

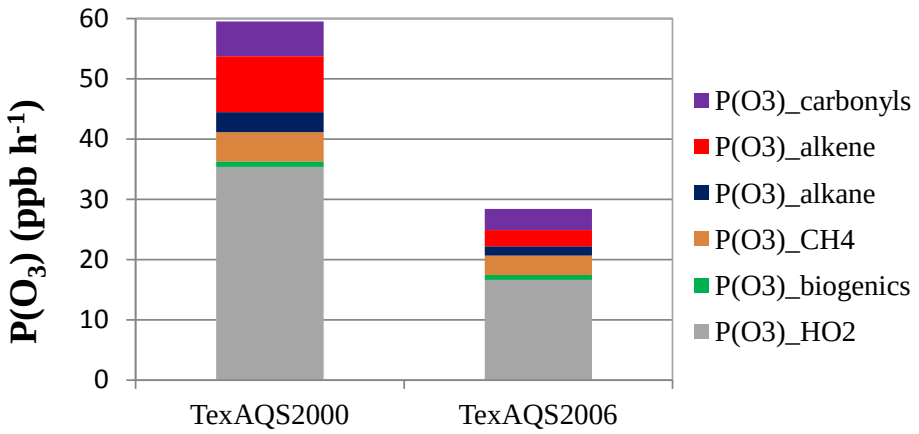

Fig. 10. The contribution of HO_2 and RO_2 radicals to $P(O_3)$ in the high $P(O_3)$ samples (average: 59 ppb h^{-1} in 2000 and 26 ppb h^{-1} in 2006). RO_2 radicals are grouped into five categories based on their VOC precursors.

ACPD
13, 19085–19120, 2013

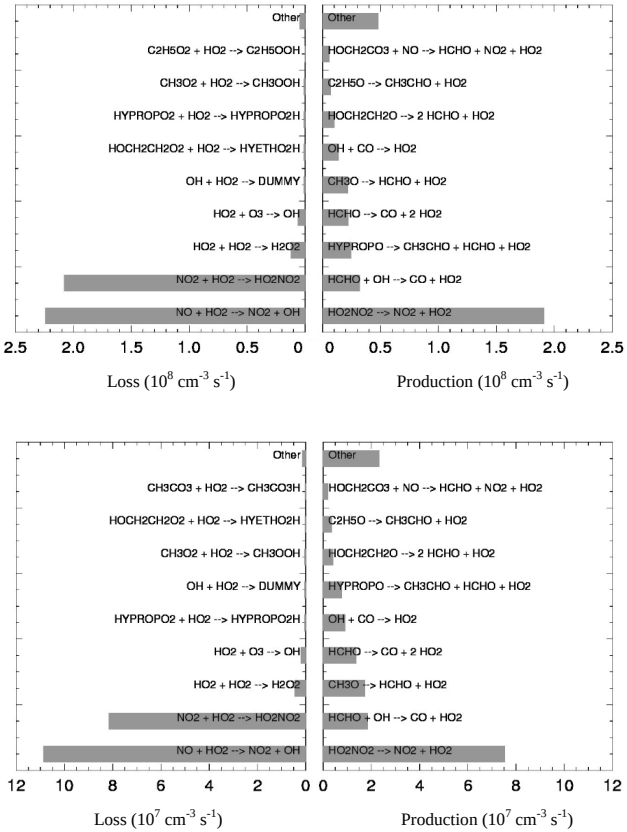

Fig. 11. Loss and production processes of HO_2 radical for high $P(O_3)$ samples. Reactions and species are from the MCM.

ACPD
13, 19085–19120, 2013

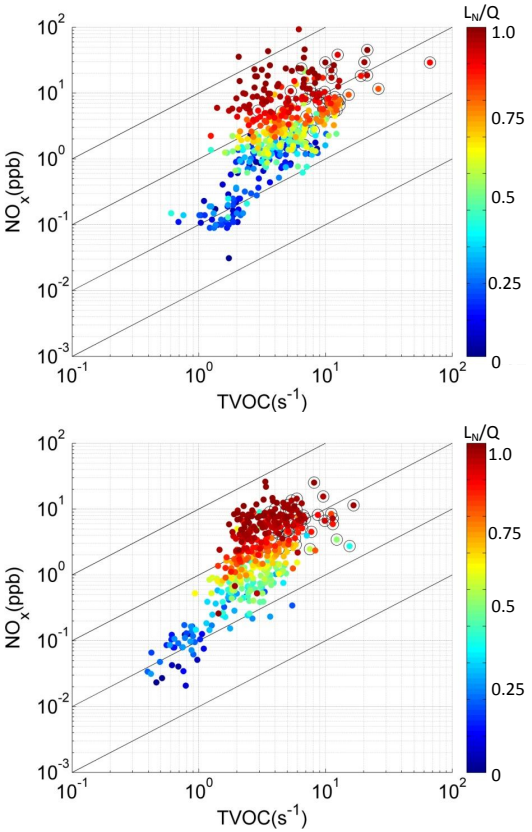

Fig. 12. The dependence of L_N/Q shown in color scale on total VOC reactivity (TVOC) and NO_x concentration for both 2000 and 2006; Samples of high $P(O_3)$ are marked by empty circles. Each diagonal line is associated with a constant TVOC to NO_x ratio (from top to bottom, $TVOC/NO_x$ = 10 : 1, 1 : 1, 1 : 10, 1 : 100).

ACPD
13, 19085–19120, 2013

CC BY

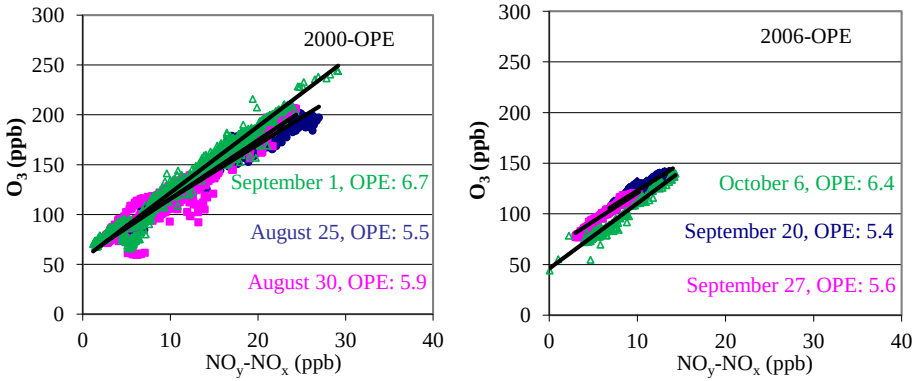

Fig. 13. The accumulative ozone production efficiency (the slope of least-square-fit between O_3 and NO_z (NO_y-NO_x) concentrations) for the three plumes with highest O_3 in 2000 (left) and 2006 (right).

ACPD
13, 19085–19120, 2013